Proceedings of the 3rd International Symposium on Uncertainty Quantification and Stochastic Modeling
D.A. Rade; A. M. G. Lima (Editors), ABCM, Maresias, SP, Brazil, February 15-19, 2016

On the Choice of Probability Density Function for the Stochastic Bonding Stiffness of Piezoelectric Structures

Heinsten F.L. Santos[1] **and Marcelo A. Trindade**[2]

[1] Institute of Agricultural Sciences and Technology, Mechanical Engineering, Federal University of Mato Grosso, Highway MT 270, Km 6, Rondonópolis, MT, 73785-901, Brazil

[2] Department fo Mechanical Engineering, São Carlos School of Engineering, University of São Paulo, Av. Trabalhador São-Carlense, 400, São Carlos, SP, 13566-590, Brazil

Abstract: A recent previous work presented an analysis of the effect of uncertainties of the bonding stiffness of the adhesive layer between a piezoceramic actuator patch and a flexible structure on the performance of such actuators for active and passive vibration control and vibration-based energy harvesting. This was done considering a stochastic model for the adhesive layer bonding stiffness based on expected statistical properties of such variable, such as expected nominal value, dispersion and positivity. The confidence intervals of the vibration control and energy harvesting performance were shown to be highly dependent on the probability density function considered for the bonding stiffness. This is due, in one hand, to the high dispersion values that can be expected for this variable and, in the other hand, to the high influence of this variable on the observed performance. This work presents the comparison between obtained performance confidence intervals when considering different, but equally reasonable, probability density functions for the adhesive layer bonding stiffness. Results are meant to confirm the need of adequate prior probability density functions, that are statistically reasonable, and provide elements that allow their selection for similar problems.

Keywords: stochastic modeling, probability density function, bonding stiffness, piezoelectric materials, active and passive vibration control

INTRODUCTION

The use of piezoelectric materials has become popular in many engineering applications. One of the most promising uses for piezoelectric materials is their incorporation into smart structures as combined sensor and actuators. In this role, the materials will be able to detect mechanical disturbances in their surroundings and adjust to these stimuli. There are basically two types of strategies adopted when it comes to integrating the piezoelectric sensors and actuators to flexible structures: bonding to the host structure's surfaces (or embedding into a laminate/composite structure) thin patches or layers of piezoelectric ceramics, polymers and/or composites. In both cases, the interface between the host structure and the piezoelectric device plays a decisive role in terms of mechanical strain and stress transfer mechanisms. A satisfactory interface ensures that effective actuation or sensing could be achieved, preventing the need of excessive voltages to be applied, in the case of actuators, and/or inaccurate output results, in the case of sensors, thereby increasing robustness of control systems.

Surface-mounted piezoelectric sensors and actuators are normally poled in the thickness direction so that the application of a through-thickness electric field forces an elongation or contraction of the actuators. Distributed sensors and actuators integrated with the flexible structure have been applied successfully in the closed-loop control. If the actuators are well-bonded to the surface of the host structure, their elongation or contraction causes a deformation of the host structure. That is why, surface-mounted piezoelectric sensors and actuators are also known as extension or extension-bending sensors and actuators and were widely used on active (Sunar and Rao, 1999), passive (Reza Moheimani, 2003) and hybrid active-passive (Tang, Liu and Wang, 2000; Trindade and Benjeddou, 2002; Santos and Trindade, 2011) control applications.

When in passive mode operation, piezoelectric materials act as energy converters, transforming strain energy into usable electrical energy. Therefore, when connected to properly designed electric circuits, they may be used for passive, semi-passive or active-passive vibration control (Hagood and von Flotow, 1991). The search for effective circuits to profit from the energy extracted from a vibrating structure by the piezoelectric device and either dissipate it into the environment or store it for future use. In both case, the energy extracted from the host structure leads to a reduction of vibratory energy and, thus, may be used for passive vibration control (Reza Moheimani, 2003). When combined to a voltage source aiming at actively control the host structure vibrations, these passive or semi-passive circuits, so-called shunt circuits, become active-passive shunt circuits (also known as active-passive piezoelectric networks). It was shown that, when properly designed, this combined solution not only allows to set either purely active or purely passive but also yields better performance than individual active or passive solutions (Tang, Liu and Wang, 2000; Santos and Trindade, 2011).

The performance of piezoelectric patches for these types of applications are very much dependent on the adequate tuning between resonant, circuit and operation frequencies and on the effective electromechanical coupling between patches and host structure. Therefore, variabilities and/or uncertainties on material properties, boundary conditions and bonding effectiveness may have a major effect on reducing the expected or predicted performance of such devices. However, few studies have attempted to analyse the effect of parametric uncertainties on active and/or passive vibration control (Santos and Trindade, 2012) and energy harvesting performance (Godoy and Trindade, 2012).

On the other hand, the effect of the bonding layer on the performance of piezoelectric sensors and actuators has not been studied extensively although most part of the research groups working in the field have shown observations that indicate a potential reduction in the transmissibility from the monitored host structure to a piezoelectric sensor and from a piezoelectric actuator to the controlled host structure. This effect is also named shear-lag effect and was studied by Sirohi and Chopra (2000) for a general piezoelectric sensor. Later, Rabinovitch and Vinson (2002) have shown that the major effect is due to stress concentrations near the edge of the bonded piezoelectric actuator. The effect of bonding stiffness was also applied for surface-bonded piezoelectric sensors and actuators focused on the electromechanical impedance of piezoelectric sensors (Bhalla et al., 2009) and on the active damping provided by piezoelectric actuators (de Faria and Almeida, 1996; Pietrzakowski, 2001). However, most bonding solutions make use of two-part Epoxy adhesives (resin and stiffener) which normally must be cured at controlled temperature to achieve the desired bonding stiffness and strength. Therefore, both mixing and curing process, not to mention intrinsic resin and stiffener properties, seem to be highly subjected to uncertainties. The effect of such uncertainties has not yet been published in the open literature.

Hence, the objective of this work is to present an analysis of the effect of uncertainties of bonding layer stiffness on the performance of piezoelectric sensors and actuators with application to passive and active shunted damping and energy harvesting. For that, the bonding layer Young modulus is represented by a stochastic parameter and Monte Carlo simulations are performed to evaluate mean and confidence intervals of the damping and energy harvesting performances.

FINITE ELEMENT MODEL OF PIEZOELECTRIC SANDWICH BEAMS

To account for the bonding layer stiffness and its effect on the performance of the piezoceramic actuator and/or sensor for vibration control and energy harvesting, a classical sandwich beam model was considered. Thus, the interface (bonding) layer between piezoceramic and host structure is allowed to present shear strains and, thus, should be able to represent the expected loss of transmissibility between outer layers (Figure 1). The three layers are assumed to be perfectly bonded and in plane stress state. Bernoulli-Euler theory is retained for the outer layers, while the bonding layer is assumed to behave as a Timoshenko beam.

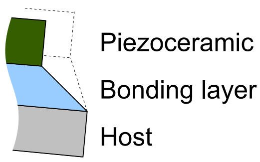

Figure 1 – Schematic representation of reduction of transmissibility due to bonding layer.

Piezoceramic layers are considered to be transversely poled and with electrodes fully covering its top and bottom skins. It is supposed that each piezoelectric layer can be connected to an electric circuit composed of inductance L_{cj}, resistance R_{cj} and voltage source V_{cj} in series. Based on these assumptions, a two-node beam finite element model was developed with four mechanical and three electrical degrees of freedom per node. The electric displacements in each layer were considered as electrical degrees of freedom. More details on the finite element model can be found in (Santos and Trindade, 2011).

Accounting for equipotentiality on electrodes covering piezoelectric patches surfaces and the relation between electric charges on circuits and patches, the structure-patches-circuits coupled equations of motion can be written as

$$\begin{bmatrix} \mathbf{M} & 0 \\ 0 & \mathbf{L}_c \end{bmatrix} \begin{Bmatrix} \ddot{\mathbf{u}} \\ \ddot{\mathbf{q}}_p \end{Bmatrix} + \begin{bmatrix} \mathbf{C} & 0 \\ 0 & \mathbf{R}_c \end{bmatrix} \begin{Bmatrix} \dot{\mathbf{u}} \\ \dot{\mathbf{q}}_p \end{Bmatrix} + \begin{bmatrix} \mathbf{K}_m & -\bar{\mathbf{K}}_{me} \\ -\bar{\mathbf{K}}_{me}^t & \bar{\mathbf{K}}_e \end{bmatrix} \begin{Bmatrix} \mathbf{u} \\ \mathbf{q}_p \end{Bmatrix} = \begin{Bmatrix} \mathbf{F} \\ \mathbf{V}_c \end{Bmatrix}, \tag{1}$$

where $\mathbf{u}$ and $\mathbf{q}_p$ are the global mechanical displacement and electric charge dofs and $\mathbf{M}$, $\mathbf{K}_m$, $\bar{\mathbf{K}}_{me}$, $\bar{\mathbf{K}}_e$ are the mass and mechanical, piezoelectric and dielectric stiffness matrices and $\mathbf{F}$ is the mechanical force vector. $\mathbf{L}_c$ and $\mathbf{R}_c$ are diagonal matrices containing the inductance and resistance and $\mathbf{V}_c$ is the vector of electric voltage applied to the electric shunt circuits. A structural damping matrix $\mathbf{C}$ can be added a posteriori.

The proposed model can be used for the analysis of applications involving for instance: i) piezoelectric actuators, that is using electric voltage applied to piezoelectric layers/patches to induce mechanical displacements, ii) piezoelectric sensors, that is using electric charge output to monitor mechanical displacements (vibrations) induced by mechanical forces, iii) piezoelectric shunted damping, that is using properly designed shunt circuits connected to the piezoelectric layers/patches to reduce mechanical vibration amplitudes, iv) piezoelectric energy harvesting, that is collecting/harvesting the electric charge induced in the piezoelectric layers/patches by the mechanical vibrations through a proper harvesting electric circuit. These cases differ mainly on the input and output considered for the analysis and how the input and/or output are processed. In all cases, due to the sandwich construction considered, the effect of a shearing bonding layer may be evaluated.

In the following, the analysis shall be divided in two parts differing mainly on the system output. In the first case, vibration control analysis, the interest is put on the reduction of transverse velocity amplitudes. In the second case, energy harvesting, the interest is put on the maximization of electric current output.

THEORETICAL DEVELOPMENT FOR VIBRATION CONTROL ANALYSIS

For vibration control analysis, the proposed model (1) is used to evaluate the mobility (velocity/force) frequency response function of the base structure. The resistive (R) or resonant (RL) shunt circuit affects both the passive and active-passive (hybrid) control performance. In the hybrid control case, besides the resistance and inductance of the shunt circuit, the active control law also determines the overall performance.

Evaluation of mechanical output under electrical and mechanical excitation

For a purely mechanical excitation, such that $\mathbf{V}_c = 0$ and $\mathbf{F} = \mathbf{b}\tilde{f}e^{\mathrm{j}\omega t}$, the amplitude of a displacement output $y = \mathbf{c}_y\mathbf{u}$ can be written such that $\tilde{y} = G_p(\omega)\tilde{f}$, where the FRF $G_p(\omega)$ is

$$G_p(\omega) = \mathbf{c}_y\{-\omega^2\mathbf{M} + \mathrm{j}\omega\mathbf{C} + \mathbf{K}_m - \bar{\mathbf{K}}_{me}(-\omega^2\mathbf{L}_c + \mathrm{j}\omega\mathbf{R}_c + \bar{\mathbf{K}}_e)^{-1}\bar{\mathbf{K}}_{me}^{\mathrm{t}}\}^{-1}\mathbf{b}, \tag{2}$$

from which, it is possible to notice that the resistance and inductance have the effect of changing the dynamic stiffness of the structure. Two particular cases of interest can be derived: i) open-circuit when $\mathbf{R}_c \to \infty$ and ii) short-circuit when $\mathbf{L}_c = \mathbf{R}_c = 0$, in which cases

$$G_p^{OC}(\omega) = \mathbf{c}_y\left\{-\omega^2\mathbf{M} + \mathrm{j}\omega\mathbf{C} + \mathbf{K}_m\right\}^{-1}\mathbf{b}, \quad G_p^{SC}(\omega) = \mathbf{c}_y\left\{-\omega^2\mathbf{M} + \mathrm{j}\omega\mathbf{C} + \mathbf{K}_m - \bar{\mathbf{K}}_{me}\bar{\mathbf{K}}_e^{-1}\bar{\mathbf{K}}_{me}^{\mathrm{t}}\right\}^{-1}\mathbf{b}. \tag{3}$$

As expected, no structural modification is observed in the open-circuit case while, for the short-circuit case, the stiffness of the piezoelectric patches is reduced.

For a purely electric excitation using a single pair patch-circuit, such that $\mathbf{F} = 0$ and $V_c = \tilde{V}_c e^{\mathrm{j}\omega t}$, the FRF between the output y and the applied voltage V_c is such that $\tilde{y} = G_c(\omega)\tilde{V}_c$, where

$$G_c(\omega) = \mathbf{c}_y\{-\omega^2\mathbf{M} + \mathrm{j}\omega\mathbf{C} + \mathbf{K}_m - \bar{\mathbf{K}}_{me}(-\omega^2 L_c + \mathrm{j}\omega R_c + \bar{K}_e)^{-1}\bar{\mathbf{K}}_{me}^{\mathrm{t}}\}^{-1}\bar{\mathbf{K}}_{me}(-\omega^2 L_c + \mathrm{j}\omega R_c + \bar{K}_e)^{-1} \tag{4}$$

In this case, the resistance and inductance of the electric circuit have two effects. The first is a modification on the dynamic stiffness of the structure as in the previous case. The second is a modification of amplitude of the equivalent force input induced in the structure by the applied voltage, which for a properly adjusted circuit can lead to a desirable amplification of the control authority of the pair patch-circuit. The particular case of a simple voltage actuator can be derived by making $L_c = R_c = 0$, for which

$$G_c^V(\omega) = \mathbf{c}_y\left\{-\omega^2\mathbf{M} + \mathrm{j}\omega\mathbf{C} + \mathbf{K}_m - \bar{\mathbf{K}}_{me}\bar{\mathbf{K}}_e^{-1}\bar{\mathbf{K}}_{me}^{\mathrm{t}}\right\}^{-1}\bar{\mathbf{K}}_{me}\bar{\mathbf{K}}_e^{-1} \tag{5}$$

For the passive control case, the shunt circuit parameters (resistance and inductance) may be designed using the standard dynamic vibration absorber theory as presented in previous works (Hagood and von Flotow, 2001; Godoy and Trindade, 2011; Santos and Trindade, 2011; Thomas, Ducarne and Deü, 2012).

Active vibration control using piezoelectric actuators and state feedback

A state feedback LQR (Linear Quadratic Regulator) optimal control is considered. For that, it is necessary to rewrite the equations of motion (1) in state space form, such that a vector of state variables $\mathbf{z}$ is defined, containing the modal displacements and velocities of a series of vibration modes of interest and the electric displacements of the piezoelectric patches and their time-derivatives. This leads to

$$\dot{\mathbf{z}} = \hat{\mathbf{A}}\mathbf{z} + \hat{\mathbf{B}}\mathbf{V}_c + \hat{\mathbf{B}}_f\mathbf{f}\,,\ \mathbf{y} = \hat{\mathbf{C}}_y\mathbf{z}, \tag{6}$$

where

$$\mathbf{z}=\begin{bmatrix}\alpha\\ \mathbf{q}_p\\ \dot{\alpha}\\ \dot{\mathbf{q}}_p\end{bmatrix},\ \hat{\mathbf{A}}=\begin{bmatrix}\mathbf{0} & \mathbf{0} & \mathbf{I} & \mathbf{0}\\ \mathbf{0} & \mathbf{0} & \mathbf{0} & \mathbf{I}\\ -\boldsymbol{\Omega}^2 & \mathbf{K}_p & -\boldsymbol{\Lambda} & \mathbf{0}\\ \mathbf{L}_c^{-1}\mathbf{K}_p^{\mathrm{t}} & -\boldsymbol{\Omega}_e^2 & \mathbf{0} & -\boldsymbol{\Lambda}_e\end{bmatrix},\quad \hat{\mathbf{B}}=\begin{bmatrix}\mathbf{0}\\ \mathbf{0}\\ \mathbf{0}\\ \mathbf{L}_c^{-1}\end{bmatrix},\ \hat{\mathbf{B}}_f=\begin{bmatrix}\mathbf{0}\\ \mathbf{0}\\ \mathbf{b}_\phi\\ \mathbf{0}\end{bmatrix},\ \hat{\mathbf{C}}_y=\begin{bmatrix}\mathbf{c}_\phi & \mathbf{0} & \mathbf{0} & \mathbf{0}\end{bmatrix}. \tag{7}$$

The modal displacements are such that $\mathbf{u}=\boldsymbol{\phi}\boldsymbol{\alpha}$ and, for mass normalized vibration modes, $\boldsymbol{\Omega}^2=\boldsymbol{\phi}^{\mathrm{t}}\mathbf{K}_m\boldsymbol{\phi}$ and $\boldsymbol{\Lambda}=\boldsymbol{\phi}^{\mathrm{t}}\mathbf{C}\boldsymbol{\phi}$. $\boldsymbol{\Omega}$ is a diagonal matrix which elements are the undamped natural frequencies of the structure with piezoelectric patches in open-circuit. $\boldsymbol{\Omega}_e^2=\mathbf{L}_c^{-1}\bar{\mathbf{K}}_e$ and $\boldsymbol{\Lambda}_e=\mathbf{L}_c^{-1}\mathbf{R}_c$ are both diagonal matrices which elements stand, respectively, for the squared natural frequencies of the electric circuits and the ratio between the resistances and inductances. The electromechanical coupling stiffness matrix projected in the undamped modal basis is defined as $\mathbf{K}_p=\boldsymbol{\phi}^{\mathrm{t}}\bar{\mathbf{K}}_{me}$. Input $\mathbf{b}$ and output $\mathbf{c}_y$ distribution vectors are also defined, with modal projections $\mathbf{b}_\phi=\boldsymbol{\phi}^{\mathrm{t}}\mathbf{b}$ and $\mathbf{c}_\phi=\mathbf{c}_y\boldsymbol{\phi}$, and $\mathbf{f}$ is a vector of the amplitudes of each mechanical force applied to the structure.

A linear state feedback for the applied voltages $\mathbf{V}_c$ is assumed such that $\mathbf{V}_c=-\mathbf{g}\mathbf{z}=-\mathbf{g}_{dm}\boldsymbol{\alpha}-\mathbf{g}_{de}\mathbf{q}_p-\mathbf{g}_{vm}\dot{\boldsymbol{\alpha}}-\mathbf{g}_{ve}\dot{\mathbf{q}}_p$, where $\mathbf{g}$ is a matrix of control gains for each state variable. Therefore, the state space equation (6) becomes

$$\dot{\mathbf{z}}=(\hat{\mathbf{A}}-\hat{\mathbf{B}}\mathbf{g})\mathbf{z}+\hat{\mathbf{B}}_f\mathbf{f}\,,\ \mathbf{y}=\hat{\mathbf{C}}_y\mathbf{z}. \tag{8}$$

For a single-input mechanical excitation f, the closed-loop or controlled amplitude of a single displacement output y can be written such that $\tilde{y}=G_h(\omega)\tilde{f}$, where the FRF $G_h(\omega)$ is

$$G_h(\omega)=\hat{\mathbf{C}}_y(\mathrm{j}\omega\mathbf{I}-\hat{\mathbf{A}}+\hat{\mathbf{B}}\mathbf{g})^{-1}\hat{\mathbf{B}}_f, \tag{9}$$

which can also be derived from the second order equations of motion projected into the undamped modal basis leading to

$$G_h(\omega)=\mathbf{c}_\phi\left\{-\omega^2\mathbf{I}+\mathrm{j}\omega(\boldsymbol{\Lambda}+\mathbf{K}_p\mathbf{D}_{cc}^{-1}\mathbf{g}_{vm})+[\boldsymbol{\Omega}^2+\mathbf{K}_p\mathbf{D}_{cc}^{-1}(\mathbf{g}_{dm}-\mathbf{K}_p^{\mathrm{t}})]\right\}^{-1}\mathbf{b}_\phi, \tag{10}$$

where the closed-loop dynamic stiffness of the electric circuit $\mathbf{D}_{cc}$ is

$$\mathbf{D}_{cc}=-\omega^2\mathbf{L}_c+\mathrm{j}\omega(\mathbf{R}_c+\mathbf{g}_{ve})+(\bar{\mathbf{K}}_e+\mathbf{g}_{de}). \tag{11}$$

In this work, the control gain $\mathbf{g}$ is calculated using the standard optimal LQR control theory applied to a single-input/single-output case, that is with only one active-passive patch-circuit pair for the control to minimize the vibration amplitude at one specific location of the structure, such that the following objective function is minimized

$$J=\frac{1}{2}\int_0^\infty\left(\dot{y}^2+rV_c^2\right)\,\mathrm{d}t, \tag{12}$$

where $\dot{y}$ is the velocity at one location of interest and V_c is the control voltage applied to the active-passive shunt circuit. The weighting factor r is automatically adjusted to guarantee a maximum control voltage of 200 V in all cases following an iterative routine proposed in (Trindade, Benjeddou and Ohayon, 1999).

STOCHASTIC MODELING OF BONDING STIFFNESS FOR UNCERTAINTY QUANTIFICATION

This section presents an approach for analyzing random uncertainties for the bonding stiffness main parameter, that is the effective Young's modulus E_b of the adhesive. This is done considering the Young's modulus as a stochastic variable, respecting a given probability density function. Random realizations of the stochastic variable E_b are then generated. Then, four analyses are performed in which, for each realization of the stochastic variable, a frequency response function of interest was evaluated.

First, the effect of the uncertainties on the passive shunted damping performance was evaluated by analyzing the realizations of $G_p(\omega)$, using (2). Then, the active-passive (hybrid) control performance was analyzed through the realizations of $G_h(\omega)$. This last analysis was divided in two cases, where the active control gain is considered either fixed or updated (to the system realization).

In all cases, 5000 Monte Carlo simulations were performed. The realizations of the frequency response functions, at any given frequency point, were used to evaluate their mean values and 95% confidence intervals, using the 2.5% and 97.5% percentiles of the realizations. The general computational procedure is schematically represented in Figure 2.

It should be noted that the probability density function for the adhesive Young's modulus is not known a priori. Furthermore, it is not viable to perform the amount of experimental measurements required to have sufficient samples

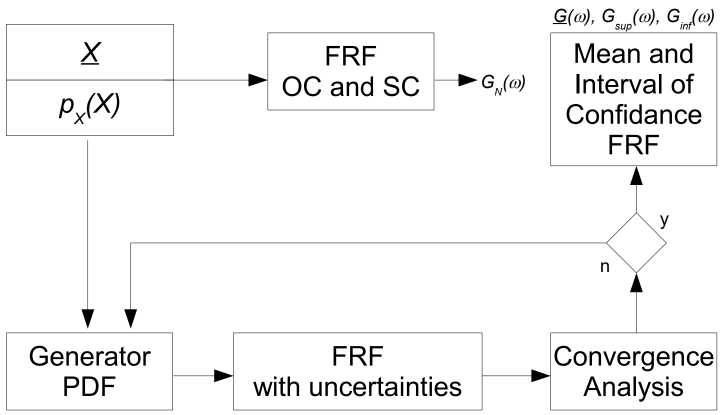

Figure 2 – Schematic representation of the computational procedure to obtain the confidence intervals for the frequency response functions $G_p(\omega)$ and $G_h(\omega)$.

to characterize its probability density function, since the bonding stiffness depends not only on a manual mixture of two components (resin and hardener) but also on a manual assembling procedure of structure, adhesive and piezoelectric patch. Therefore, the effective bonding stiffness would have to be characterized after assembling.

Nevertheless, it is expected that a mean (or nominal) value could be estimated and, also, that it should be positive. Therefore, using the Maximum Entropy Principle (Jaynes, 1957; Soize, 2001), a reasonable stochastic model can be constructed from a Gamma probability density function (pdf), such that

$$p_E(E) = \mathbb{I}_{]0,+\infty[}\left(\frac{1}{\delta_E^2\bar{E}}\right)^{\delta_E^{-2}} \frac{E^{\delta_E^{-2}-1}}{\Gamma(\delta_E^{-2})}\exp\left(-\frac{E}{\delta_E^2\bar{E}}\right), \tag{13}$$

in which $\delta_E = \sigma_E/\bar{E}$ is the relative dispersion of stochastic bonding layer Young's modulus E_b and σ_E is its standard deviation. The Gamma function is defined as $\Gamma(x) = \int_0^\infty t^{x-1}e^{-t}\mathrm{d}t$.

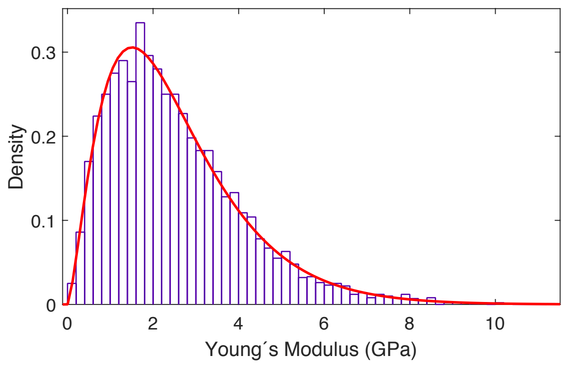

Figure 3 – Histogram of sample generated using gamrnd and 5000 realizations.

An amount of 5000 realizations of the stochastic modulus were generated using MATLAB function *gamrnd*, considering a mean value of 2.5 GPa and a relative dispersion of 100 %. The histogram shown in Figure 3 follows very closely the expected behavior of a Gamma pdf with only positive values. However, it was observed that for this large value of relative dispersion, there is a concentration of realizations below 2 GPa. This means that the Gamma pdf displaces substantially the most probable value from the nominal value towards zero (Figure 3). This behavior will have a direct effect on the output distribution, namely the distribution of passive, active and active-passive control performance subject to the uncertainties of the bonding stiffness. Therefore, two other pdf were considered to represent the bonding stiffness, namely a Beta pdf and a truncated Gaussian pdf.

The Beta probability density function may also be obtained from the Maximum Entropy Principle, considering that the stochastic variable is positive but also bounded. The general description of the Beta pdf for a stochastic variable bounded between 0 and 1 is given by (Ritto, Soize and Sampaio, 2010)

$$p_X(X) = \mathbb{I}_{]0,1[}(X)\frac{\Gamma(\alpha+\beta)}{\Gamma(\alpha)\Gamma(\beta)}X^{\alpha-1}(1-X)^{\beta-1}, \tag{14}$$

where α and β are two parameters assuming only positive values. They are related to the mean value and relative dispersion such that

$$\alpha = \frac{\bar{X}}{\delta_X^2}\left(\frac{1}{\bar{X}} - \delta_X^2 - 1\right), \; \beta = \frac{\bar{X}}{\delta_X^2}\left(\frac{1}{\bar{X}} - \delta_X^2 - 1\right)\left(\frac{1}{\bar{X}} - 1\right). \tag{15}$$

The mean value $\bar{X}$ and relative dispersion δ_X of the normalized stochastic variable X must be written in terms of the actual mean and relative dispersion of the adhesive Young's modulus, $\bar{E}$ and δ_E, such that

$$\bar{X} = \frac{\bar{E}-E_1}{E_2-E_1}, \; \delta_X = \sqrt{\frac{\bar{E}(\delta_E^2+1)-(\bar{E}-E_1)^2-2E_1(\bar{E}-E_1)-E_1^2}{(\bar{E}-E_1)^2}} \tag{16}$$

As performed previously for the Gamma pdf, 5000 realizations were generated for the Beta pdf using MATLAB function *betarnd*, considering $\bar{E} = 2.5$ GPa, $\delta_E = 52\%$, $E_1 = 0.1$ GPa and $E_2 = 4.9$ GPa, which leads to $\alpha = 1.2$ and $\beta = 1.2$. Figure 4 shows the histogram of the sample generated with these parameters.

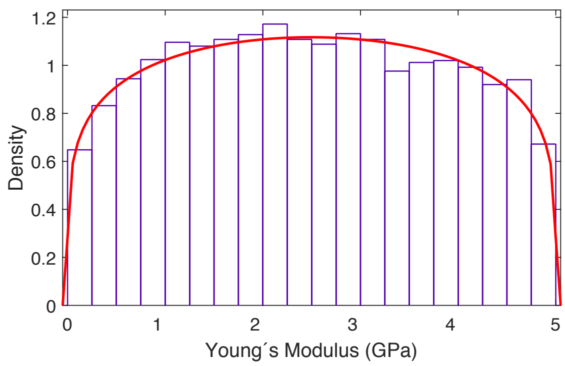

Figure 4 – Histogram of sample generated with betarnd and 5000 realizations.

Another probability density function considered for the adhesive Young's modulus is the Truncated Gaussian pdf. The Gaussian pdf, also known as Normal pdf, is given by

$$p_E(E) = \mathbb{I}_{]-\infty,+\infty[}(E)\frac{1}{\sigma_E\sqrt{2\pi}}e^{-\frac{(E-\bar{E})^2}{2\sigma_E^2}} \tag{17}$$

Notice that the support of the Gaussian pdf is $]-\infty,+\infty[$ and, thus, it may lead to negative values for the adhesive Young's modulus. Therefore, it may be necessary to truncate the pdf in order to admit only positive values. 5000 realizations were generated for the Gaussian pdf using MATLAB function *normrnd*, considering $\bar{E} = 2.5$ GPa, $\delta_E = 94\%$. Figure 5 shows the histogram of the sample generated with these parameters. In this case, no need to truncate the pdf was observed since all realizations were inside the acceptable range, $]0,5[$ GPa.

UNCERTAINTY QUANTIFICATION RESULTS

A cantilever beam with surface-mounted piezoceramic, as shown in Figure 6, was analyzed in order to evaluate the APPN performance in terms of passive damping, control authority and active-passive damping. The extension piezoceramics are made of PZT-5H material whose properties are: $\bar{C}_{11}^D = 97.767$ GPa, $\bar{C}_{33}^D = 119.71$ GPa, $C_{55}^D = 42.217$ GPa, $\rho = 7500\ kg\ m^{-3}$, piezoelectric coupling constant $\bar{h}_{31} = -1.3520$ N C^{-1}, and dielectric constant $\beta_{33}^{\bar{\varepsilon}} = 57.83010^6$ m F^{-1}. For the Aluminium beam using a two-part Epoxy bounding layer. Its material properties were considered to be deterministic: density 1160 $kg\ m^{-3}$, nominal value of Young Modulus 2.5 GPa and Poisson ration 0.4. In addition, a constant viscous modal damping of 0.5% were considered. The resistance and inductance were tuned to the first resonance frequency, using an optimization algorithm, leading to $R_c = 13984\ \Omega$ and $L_c = 283.42\ H$. The purely passive action is obtained by eliminating the voltage source and the purely active action is obtained by making $R_c = L_c = 0$. For the general case, the inductance and resistance not only modify the dynamic stiffness of the structure, leading to damping and/or absorption, but also affects the active control authority of the actuator.

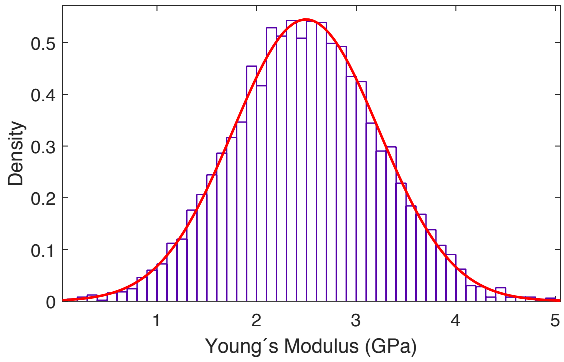

Figure 5 – Histogram of sample generated with normrnd and 5000 realizations.

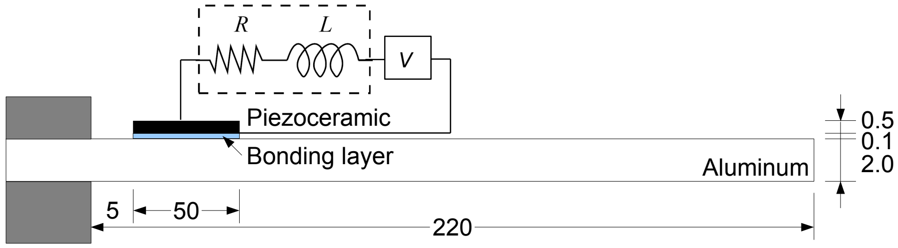

Figure 6 – Representation of cantilever beam with bonded extention piezoceramic patch.

Gamma Probability Density Function

The Figure 7, can be observed the first mode from configuration presented in Figure 6 using the $p.d.f$ Gamma developed in Figure 3. For this configuration, the Figure $7(a)$ shows the mean and 95 % confidence interval for the frequency response of the shunted cantilever beam subjected to uncertainties of bonding layer stiffness compared to the short-circuit condition (without passive control).The interval of confidence presented an alteration on the resonance, making the peak of resonance displaced to the left, this represent more values lower 2.5 GPa in the Gamma probability density function. May notice that the nominal model indicates a passive reduction in the vibration amplitude of 20 dB (considering the difference between peak responses for SC and RL), while when considering the uncertainties is found to be in the range 18 dB for superior or 22 dB for inferior bound.

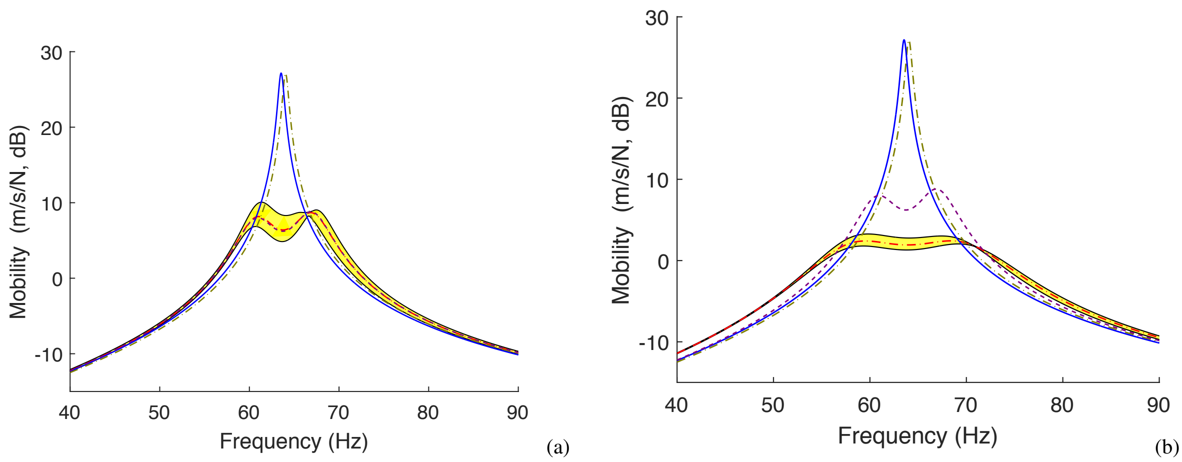

Figure 7 – Confidence interval for a Gamma Probability Density Function Gamma.(a) Purely Passive Control, (b) Active Passive Piezoelectric Network

The same analysis considering the Figure $7(b)$ a reduction the confidence interval and a more stable behavior. This can be explained because the active control in the configuration. When compare the superior bound and the structure connected with the open circuit, can be observed a reduction of 22 dB and 23 dB when compare with the values for optimal Resistance and Inductance in Active Passive Piezoelectric Network.

Beta Probability Density Function

The Figure 8, can be observed the first mode from configuration presented in Figure 6 using the $p.d.f$ Beta developed in Figure 4. For this configuration, the Figure $8(a)$ shows the mean and 95 % confidence interval for the frequency response of the shunted cantilever beam subjected to uncertainties of bonding layer stiffness compared to the short-circuit condition (without passive control).The interval of confidence presented an alteration on the resonance, making the peak of resonance displaced to the left, this represent more values lower 2.5 GPa in the Gamma probability density function. May notice that the nominal model indicates a passive reduction in the vibration amplitude of 20 dB (considering the difference between peak responses for SC and RL), while when considering the uncertainties is found to be in the range 7 dB for superior or 22 dB for inferior bound.

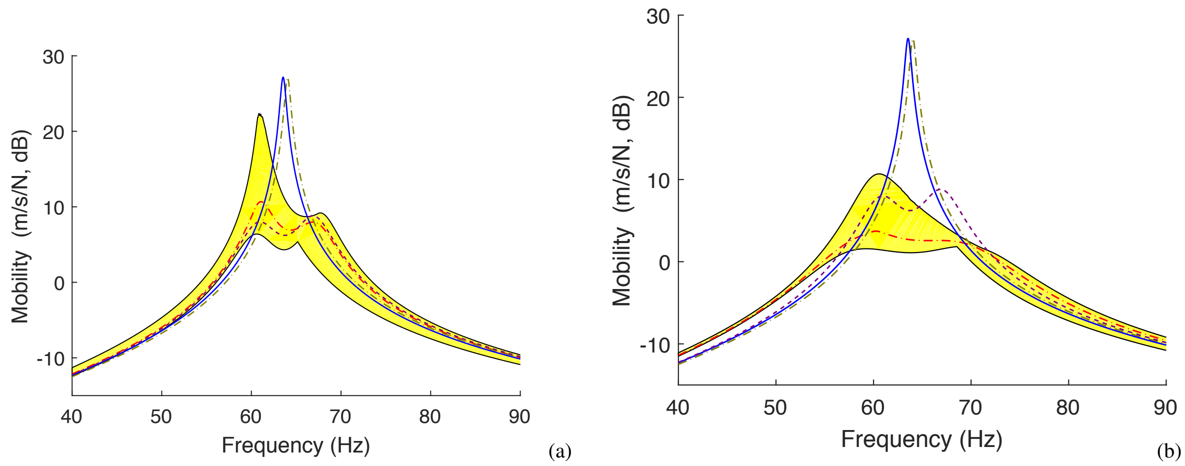

Figure 8 – Confidence interval for a Beta Probability Density Function.(a) Purely Passive Control, (b) Active Passive Piezoelectric Network

The same analysis considering the Figure $8(b)$ a reduction the confidence interval and a more stable behavior. This can be explained because the active control in the configuration. When compare the superior boundary and the structure connected with the open circuit, can be observed a reduction of 17 dB and 24 dB when compare with the mean values of the interval confidence.

Norm Probability Density Function

The Figure 9, can be observed the first mode from configuration presented in Figure 6 using the $p.d.f$ Normal developed in Figure 5. For this configuration, the Figure $9(a)$ shows the mean and 95 % confidence interval for the frequency response of the shunted cantilever beam subjected to uncertainties of bonding layer stiffness compared to the short-circuit condition (without passive control). The interval of confidence presented an alteration on the resonance, making the peak of resonance displaced to the left, this represent more values lower 2.5 GPa in the Normal probability density function. May notice that the nominal model indicates a passive reduction in the vibration amplitude of 20 dB (considering the difference between peak responses for SC and RL), while when considering the uncertainties is found to be in the range 17.5 dB for superior or 21 dB for inferior bound.

Realizing the same analysis considering the Figure $9(b)$ a reduction the confidence interval and a more stable behavior. This can be explained because the active control in the configuration. When compare the superior boundary and the structure connected with the open circuit, can be observed a reduction of 23 dB and 24 dB when compare with the values for optimal Resistance and Inductance in Active Passive Piezoelectric Network.

Intervals of Confidence

The vibration performance of interval confidence presented in Figure 10 shows the influence of dispersion for different probability functions. The Gamma $p.d.f.$, obtained generated using MATLAB function with relative dispersion of 100 %, present a interval confidence lower when compare with the Beta $p.d.f.$ also generated using MATLAB function with $\delta_E = 52$ %. The same effect was observed when compare the Beta $p.d.f$ and the Normal $p.d.f$ with $\delta_E =$ 94 %, the interval of confidence is lower when compare with the Beta $p.d.f$. For cases represented in 10(b) may observed that the LQR control combined with the resonant shunt circuit presents the same behavior, but the Beta $p.d.f$ present values affecting the tuning between resonant device and target frequency to control and also the transmissibility.

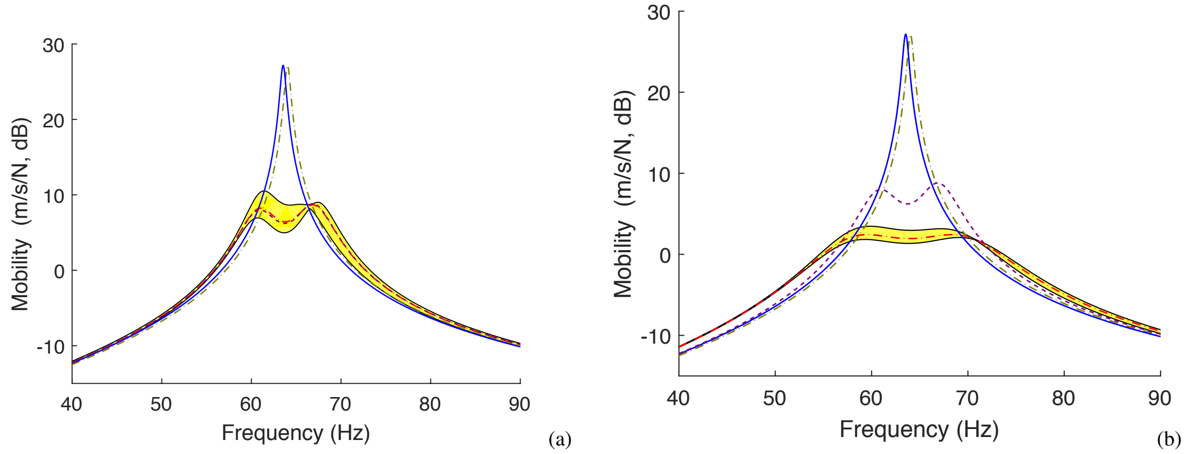

Figure 9 – Confidence interval for a Norm Probability Density Function.(a) Purely Passive Control, (b) Active Passive Piezoelectric Network

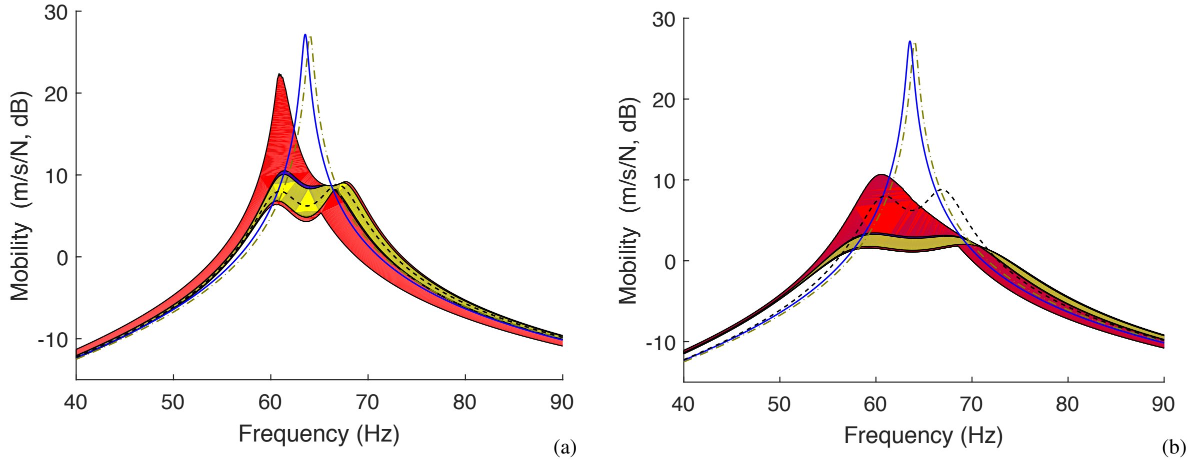

Figure 10 – Comparasion of the intervals of confidence for all $p.d.f.$'s developed

CONCLUSION

An analysis of the effect of uncertainties of the bonding layer stiffness on the piezoelectric vibration control was performed. For passived (shunted) vibration control, bonding stiffness uncertainties mainly affect the tunning between electric circuit and piezo-structure and, thus, reducing the overall performance. For active-passive vibration contol, they may also affect the control gain design. The active-passive control still outperforms the purely passive case and both passive and active-passive still seem to perform quite well even under the considered bonding stiffness uncertainties.

ACKNOWLEDGEMENTS

Support of MCT/CNPq/FAPEMIG National Institute of Science and Technology on Smart Structures in Engineering, grant 574001/2008-5, and National Council for Scientific and Technological Development (CNPq), grants 306675/2011-0 and 309193/2014-1, is acknowledged.

REFERENCES

Bhalla S., Kumar P., Gupta A. and Datta T.K. Simplified impedance model for adhesively bonded piezo-impedance transducers. *Journal of Aerospace Engineering*, 22(4):373–382, 2009.

De Faria, A.R. and Almeida, S.F.M. Modeling of actively damped beams with piezoelectric actuators with finite stiffness bond. *Journal of Intelligent Material Systems and Structures*, 7(6):677–688, 1996.

Godoy T.C. and Trindade, M.A. Modeling and analysis of laminate composite plates with embedded active-passive piezoelectric networks. *Journal of Sound and Vibration*, 330:194–216, 2011.

Godoy T.C. and Trindade, M.A. Effect of parametric uncertainties on the performance of a piezoelectric energy harvesting device. *Journal of the Brazilian Society of Mechanical Sciences and Engineering*, 34(SI2):552–560, 2012.

Hagood, N.W. and von Flotow A. Damping of structural vibrations with piezoelectric materials and passive electrical networks. *Journal of Sound and Vibration*, 146(2):243–268, 1991.

JAynes, E.T. Information theory and statistical mechanics. *Physical Review*, 106(4):620–630, 1957.

Pietrzakowski, M. Active damping of beams by piezoelectric system: effects of bonding layer properties. *International Journal of Solids and Structures*, 38:7885–7897, 2001.

Rabinovitch O. and Vinson J.R. Adhesive layer effects in surface-mounted piezoelectric actuators. *Journal of Intelligent Materials Systems and Structures*, 13:689–704, 2002.

Reza Moheimani S.O. A survey of recent innovations in vibration damping and control using shunted piezoelectric transducers. *IEEE Transactions on Control Systems Technology*, 11(4):482–494, 2003.

Ritto T.G., Soize, C. and Sampaio, R. Stochastic dynamics of a drill-string with uncertain weight-on-hook. *Journal of the Brazilian Society of Mechanical Sciences and Engineering*, 32(3):250–258, 2010.

Santos, H.F.L. and Trindade, M.A. Structural vibration control using extension and shear active-passive piezoelectric networks including sensitivity to electrical uncertainties. *Journal of the Brazilian Society of Mechanical Sciences and Engineering*, 33(3):287–301, 2011.

Santos, H.F.L. and Trindade, M.A. Performance of active and passive vibration control using piezoelectric materials subjected to uncertainties on electrical and material properties. *Proceedings of the 1st International Symposium on Uncertainty Quantification and Stochastic Modeling*, Maresias, 2012.

Sirohi, J. and Chopra, I. Fundamental understanding of piezo-electric strain sensors. *Journal of Intelligent Materials Systems and Structures*, 11(4):246–257, 2000.

Soize, C. Maximum entropy approach for modeling random uncertainties in transient elastodynamics. *Journal of the Acoustical Society of America*, 109(5):1979–1996, 2001.

Sunar, M. and Rao, S.S. Recent advances in sensing and control of flexible structures via piezoelectric materials technology. *Applied Mechanics Review*, 52(1):1–16, 1999.

Tang, J., Liu, Y. and Wang, K.W. Semiactive and active-passive hybrid structural damping treatments via piezoelectric materials. *The Shock and Vibration Digest*, 32(3):189–200, 2000.

Thomas O., Ducarne J. and Deü J.-F. Performance of piezoelectric shunts for vibration reduction. *Smart Materials and Structures*, 21(1):015008, 2012.

Trindade, M.A. and Benjeddou, A. Hybrid active-passive damping treatments using viscoelastic and piezoelectric materials: review and assessment. *Journal of Vibration and Control*, 8(6):699–746, 2002.

Trindade, M.A., Benjeddou, A. and Ohayon, R. Parametric analysis of the vibration control of sandwich beams through shear-based piezoelectric actuation. *Journal of Intelligent Materials Systems and Structures*, 10(5):377–385, 1999.

RESPONSIBILITY NOTICE

The authors are the only responsible for the printed material included in this paper.